Korea-Australia Rheology Journal
Vol. 14, No. 2, June 2002 pp. 49-55

Large amplitude oscillatory shear behavior of the network model for associating polymeric systems

Seung Ha Kim, Hoon Goo Sim, Kyung Hyun Ahn* and Seung Jong Lee
School of Chemical Engineering, Seoul National University, San 56-1 Shillim-dong Gwanak-gu, Seoul 151-744, Korea

(Received December 20, 2001; final revision received February 27, 2002)

Abstract

To understand the large amplitude oscillatory shear (LAOS) behavior of complex fluids, we have investigated the flow behavior of a network model in the LAOS environment. We applied the LAOS flow to the model proposed by Vaccaro and Marrucci (2000), which was originally developed to describe the system of associating telechelic polymers. The model was found to predict at least three different types of LAOS behavior; strain thinning (G' and G" decreasing), strong strain overshoot (G' and G" increasing followed by decreasing), and weak strain overshoot (G' decreasing, G" increasing followed by decreasing). The overshoot behavior in the strain sweep test, which is often observed in some complex fluid systems with little explanation, could be explained in terms of the model parameters, or in terms of the overall balance between the creation and loss rates of the network junctions, which are continually created and destroyed due to thermal and flow energy. This model does not predict strain hardening behavior because of the finitely extensible nonlinear elastic (FENE) type nonlinear effect of loss rate. However, the model predicts the LAOS behavior of most of the complex fluids observed in the experiments.

Keywords : large amplitude oscillatory shear (LAOS), complex fluid, network model

1. Introduction

Complex fluids are used in many fields of industry, which are related with foods, personal care products, electronic and optical materials and many biological applications, for example. The rheological properties of a complex fluid are closely related with its microstructure (Larson, 1999). Among many rheological measurements, dynamic test or small amplitude oscillatory shear (SAOS) has been most widely used because it is sensitive to the microstructure and has sound mathematical backgrounds (Macosko, 1994). In many cases, the dynamic test is sensitive enough to distinguish structural difference even in nanometer scale or any subtle structural change evolved during the processing. However, the SAOS test can be used only at very small strain enough to guarantee the linear viscoelasticity because it is based on the linear viscoelasticity theory.

As the strain increases, the stress is not sinusoidal any more, and the behavior can no longer be described in terms of the storage modulus and the loss modulus due to the higher harmonic contributions (Dealy and Wissbrun, 1990). The dynamic test in the nonlinear region is often called a large amplitude oscillatory shear (LAOS) test because the strain amplitude is not small any more. The LAOS behavior has been studied in depth but much less than the SAOS because the nonlinear phenomenon is much more complicated and difficult to analyze (Giacomin and Oakley, 1992; Giacomin and Dealy, 1993; Yosick and Giacomin, 1996). For example, the storage or loss moduli in nonlinear region lose their mathematical background or physical meaning defined in the linear region, and cannot be treated as such. Very recently, the LAOS behavior of complex fluids is getting investigated with the concept of Fourier transformation (Wilhelm *et al.*, 1998; 1999; 2000; See, 2001). Fourier transformation decomposes a waveform or function in time domain into frequency dependent spectrum, then it sums to the original waveform with the stress response, which has been decomposed into higher harmonics in the frequency domain. More precise analysis will require the Fourier transformation analysis, however in this paper, we first investigate the LAOS behavior in a less precise way, neglecting the higher harmonic contributions as most rheometers do, to compare the results with those obtained from a strain sweep test in an actual rheometer. Recently Hyun *et al.* (2002) summarized the phenomenological observations of the LAOS behavior of complex fluids, indicating that there exist at least four types of LAOS behavior: type I, strain thinning (G', G" decreas-

*Corresponding author: ahnnet@snu.ac.kr

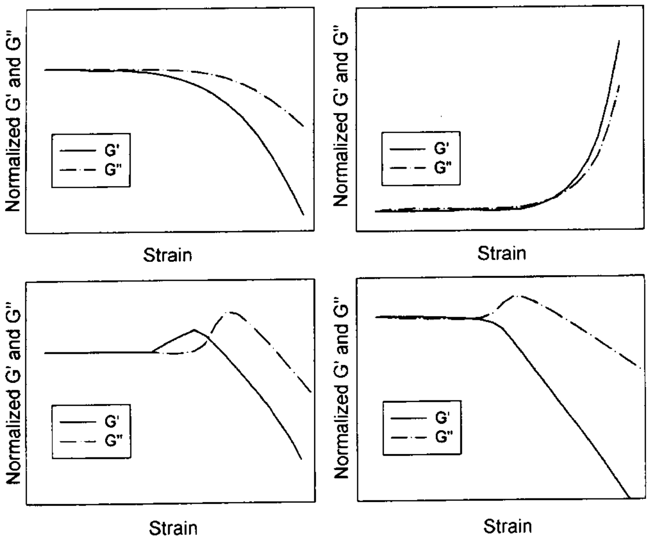

Fig. 1. Types of LAOS behavior observed in experiments: strain thinning, strain hardening, weak strain overshoot, and strong strain overshoot (clockwise from top left).

ing); type II, strain hardening (G', G'' increasing); type III, weak strain overshoot (G' decreasing, G'' increasing followed by decreasing); type IV, strong strain overshoot (G', G'' increasing followed by decreasing). Each type is reproduced in Fig. 1.

The purpose of this paper is to investigate the mechanism of such a complex behavior under large amplitude oscillatory shear. We have applied a network model as a tool to understand the behavior of complex fluids under LAOS. We have chosen a network model proposed by Vaccaro and Marrucci (2000) and performed the LAOS test. The characteristic feature of this model is that it considers pendent (dangling) chains as well as active chains, so that the model has two contributions from both active and pendent chains. We will briefly review the theoretical aspects first.

2. Theory

2.1. Basic concepts of a network model

In network models, a network is composed of segments and junctions. Segment is a part of macromolecular chain or a microstructure joining two successive junctions, and the junctions are the points where the interactions are localized. They are continually created and destroyed due to thermal and flow energy. The Lodge model, one of many network models, is the simplest and incorporates basic features common in network models, but with some assumptions. First, the interactions are localized only at isolated points. For this reason, dangling or free chains are neglected in the Lodge model. Second, the material is assumed to be incompressible, that is, we consider only deformations at constant volume. Third, the flow is homogeneous. Fourth, the segment is a Gaussian chain. As the segments are lost and created during the flow, the network consists of segments with a distribution of ages. If we let the number per unit volume of segments of length Q that are created per unit time at time t be denoted by $L_i(Q, t)$, and the probability per unit time that a segment will be destroyed by $\lambda_i^{-1}(Q, t)$, then the convection equation that determines the distribution function of the segments becomes

$$\frac{\partial \Psi_i}{\partial t} = -\frac{\partial}{\partial \boldsymbol{Q}} \cdot [\boldsymbol{\Psi}_i \boldsymbol{\kappa} \cdot \boldsymbol{Q}] + L_i(Q, t) - \frac{\Psi_i}{\lambda_i(Q, t)} \tag{1}$$

where $\boldsymbol{Q}$ is the segment vector, $\boldsymbol{\kappa}$ is the transpose of the velocity gradient tensor ($\boldsymbol{\kappa} = \nabla V^T$), and $\Psi_i(\boldsymbol{Q}, t)$ is a distribution function which is defined such that

$\Psi_i(\boldsymbol{Q}, t)d\boldsymbol{Q}$ = number of segments per unit volume at time t that have an end-to-end vector in the range of $d\boldsymbol{Q}$ about $\boldsymbol{Q}$ (2)

In this model, $L_i(Q, t)$ is the creation rate of the junctions and $\frac{\Psi_i}{\lambda_i(Q, t)}$ is the loss rate. In other network models, the main difference is the form of creation and loss rates (Bird *et al.*, 1987; Ahn and Oaski, 1995; Yosick *et al.*, 1997).

However, the model proposed by Vaccaro and Marrucci (2000) is different from most of other network models in that the effect of dangling chains is taken into account. They considered the simple case of telechelic chains, which are 3-block molecules of the form A-B-A, with B a long water-soluble polymer and A a comparatively short hydrophobic segment. The telechelic chain can be visualized as an otherwise ordinary polymer carrying two sticky points at the extremities, which tend to segregate by sticking together. In concentrated solutions, most chains form loops, while some chains have their sticky points in neighboring micelles, thus forming elastic bridges between them. They concentrated on the dynamics of the active chains, ignoring the role played by the loop chains. Active chains will occasionally become pendent when one of the two sticky points detach from the aggregate. Pendent chains will soon reattach again to the network. Therefore there are two distribution functions for the active and pendent chains respectively.

We now explain the large amplitude oscillatory shear (LAOS) test. The imposed shear strain is

$$\gamma(t) = \gamma_0 \sin(\omega t) \tag{3}$$

and the shear rate becomes

$$\dot{\gamma}(t) = \gamma_0 \cos \sin(\omega t) \tag{4}$$

Then a linear shear stress response is sinusoidal as following.

$$\sigma(t) = \sigma_0 \sin(\omega t + \delta) = \sigma_0' \sin(\omega t) + \sigma_0'' \cos(\omega t) \tag{5}$$

In the linear regime, the storage modulus G' and loss modulus G" are defined as;

$$G' = \sigma_0 \cos(\delta)/\gamma_0 = \sigma_0'/\gamma_0,\ G'' = \sigma_0 \sin(\delta)/\gamma_0 = \sigma_0''/\gamma_0 \quad (6)$$

where δ is the phase angle. When the shear strain amplitude γ_0 becomes large, the stress response is no longer sinusoidal but can be represented as a Fourier series containing multiple harmonics of stress contribution,

$$\sigma(t) = \sum_{n=1,odd}^{\infty} \sigma_n \sin(n\omega_0 t + \delta_n) \quad (7)$$

where the amplitude $\sigma_n(\omega, \gamma_0)$ of the harmonics depend on the strain amplitude and the frequency. The higher harmonic contributions to the stress tensor can be analyzed by the spectra in Fourier space with respect to their frequency. However, in this paper, we calculate the dynamic moduli as if it is done in a rheometer, neglecting the higher harmonic contributions, to compare the results with those obtained from a strain sweep test in an actual rheometer. Therefore, G' and G" at large strain can be named as the effective storage and loss moduli respectively. In this paper, G' and G" will be interchangeably used as the effective elastic modulus and the effective loss modulus for convenience afterwards.

2.2. Mathematical formulation of the Marrucci model

Vaccaro and Marrucci (2000) assumed that the sum of the number of active and pendent chains is constant.

$$\upsilon_a(t) + \upsilon_b(t) = \upsilon = \text{const} \quad (8)$$

$$y_a = \frac{\upsilon_a}{\upsilon},\ y_p = \frac{\upsilon_p}{\upsilon},\ y_a + y_p = 1 \quad (9)$$

where υ_a is the number of active chains per unit volume existing at any time t, and υ_p, the analogous quantity for pendent chains. The distribution function of active chains is assumed to be

$$\frac{\partial \psi}{\partial t} = -\frac{\partial}{\partial R}\cdot(\psi \boldsymbol{\kappa}\cdot \boldsymbol{R}) - \beta(\boldsymbol{R})\psi + \alpha(\boldsymbol{R})\varphi \quad (10)$$

where $\psi(\boldsymbol{R}, t)$ is the distribution function for the active chains and the three terms on the right-hand side result form chain deformation, detachment from the network, and attachment to the network, respectively. The distribution function of pendent chains is assumed to be

$$\frac{\partial \varphi}{\partial t} = -\frac{\partial}{\partial R}\cdot\left(-D\frac{\partial \varphi}{\partial R} + \varphi\frac{D}{kT}F(\boldsymbol{R}) + \varphi\boldsymbol{\kappa}\cdot\boldsymbol{R}\right) - \alpha(\boldsymbol{R})\varphi + \beta(\boldsymbol{R})\psi \quad (11)$$

where $\varphi(\boldsymbol{R}, t)$ is the distribution function for the pendent chains. In the pendent chains the divergence term is more complex due to thermal motion. The effect of thermal motion is considered through the diffusion terms of the end bead and the elasticity of the connecting spring. The spring force $\boldsymbol{F}$ is assumed to be

$$\boldsymbol{F}(\boldsymbol{R}) = -\frac{3kT}{Nb^2}\frac{2}{1 - R^2/(Nb)^2} \quad (12)$$

where b and N are the length and the number of Kuhn segments, respectively. The kinetic terms are written as follows

$$\alpha(\boldsymbol{R}) = \alpha_0 + \alpha_1\frac{R}{R_0} \quad (13)$$

$$\beta(\boldsymbol{R}) = \frac{\beta_0}{1 - R^2/(Nb)^2} \quad (14)$$

where $R_0 = bN^{1/2}$ is the end-to-end distance at equilibrium, and α_0, α_1 and β_0 are rate constants(dimensions of reciprocal time). The expression of the corresponding stress tensor $\boldsymbol{T}(t)$ is

$$T = \boldsymbol{T}_a + \boldsymbol{T}_p = \upsilon(\langle -FR\rangle_a + \langle -FR\rangle_p) \quad (15)$$

where $\boldsymbol{T}_a$ and $\boldsymbol{T}_p$ are the contributions of active and pendent chains, respectively.

3. Results and discussion

The Marrucci model has three parameters; two creation rate constants (α_0 and α_1) and one loss rate constant (τ or β_0^{-1}). As the creation rate constants (α_0 and α_1) increase, the number of active segment increases, while the number of active segment decreases as the loss rate constant (τ) increases. We investigated the stress response under LAOS by varying α_0 and α_1 from 5 to 20 and τ from 0.01 to 1.0. As the loss rate constant τ is related to the relaxation time, the rheological properties are supposed to show a frequency dependent behavior. The range of parameter set investigated here is wide enough to cover the diverse situations that are physically meaningful. Furthermore being the parameter set the same, the response of strain sweep depends on frequency. For this reason, we have changed the parameter set at various frequencies. By performing the strain sweep test, we have found that the model predicts four different types in LAOS behavior. Three types out of four reproduce the LAOS behavior observed in experiments and one looks unphysical.

Type A (Strain thinning)

This type appears when α_0 is large, α_1 is zero and τ is small. In addition this type appears only when the imposed frequency is smaller than the crossover frequency. In these cases, the effective storage modulus and the effective loss modulus decrease as the strain amplitude increases beyond the critical strain, while they are constant at small strain. This pattern is shown in Fig. 2. This is the typical behavior of strain sweep results of most polymer solutions or melts. Because the chain of polymer solutions or melts is in a

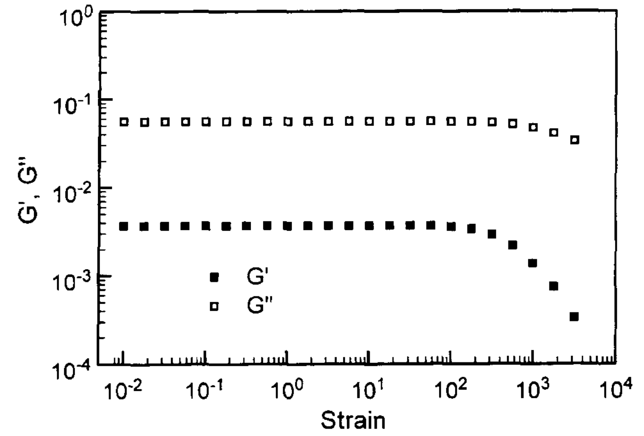

Fig. 2. Type A: strain thinning (with parameter set α_0=5, α_1=0, τ=0.01, at frequency 0.01).

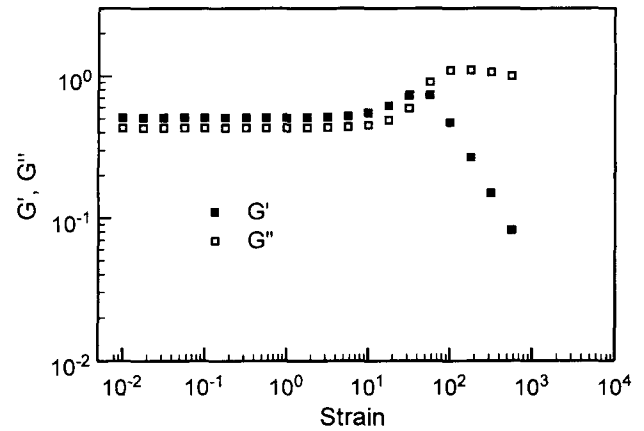

Fig. 3. Type B: strong strain overshoot (with parameter set α_0=1, α_1=5, τ=0.01, at frequency=0.178).

state of entanglement at small strain, the storage and the loss modulus remain constant in linear region. The creation rate remains constant as strain increases because the creation rate in this case does not depend on end-to-end distance R, while the loss rate become larger than the creation rate as strain increases. Hence, the parameter set leads to strain thinning behavior as the strain amplitude increases.

Type B (Strong strain overshoot)

When α_1 is larger than α_0 and τ is small, both G' and G" show an overshoot at intermediate strain amplitude near the crossover frequency as shown in Fig. 3. When α_1 is larger than α_0, the creation rate becomes larger as the strain amplitude increases, and the loss rate increases too. As a result of the balance between the creation and loss rates, there appears an overshoot at intermediate strain amplitude. However the moduli decrease at larger strain as the loss rate becomes more dominant due to the FENE (Finitely Extensible Nonlinear Elastic) type nonlinear effect of loss rate. A hydrophobically modified alkali-

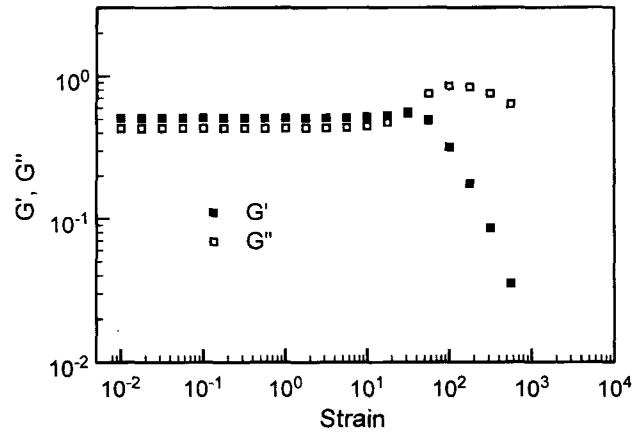

Fig. 4. Type C: weak strain overshoot (with parameter set α_0=5, α_1=1, τ=0.01, at frequency=0.178).

swellable associative polymer (HASE) system is known to show the behavior of this type (Tirtaatmadja *et al.*, 1997).

Type C (Weak strain overshoot)

When α_0 is larger than α_1 and τ is small, the effective storage modulus G' decreases with strain, but the effective loss modulus G" has an overshoot as shown in Fig. 4. When α_0 is larger than α_1, the creation rate has a weaker dependence of strain amplitude than the case of type B, and the creation rate increases slowly while the loss rate increases faster than the creation rate as the strain amplitude increases. As the creation term in this case is smaller than that of type B, the overall balance between the creation and loss rates in this case leads to weaker hardening effect than the former case. As a consequence, only G" shows an overshoot. Both G' and G" decrease at larger strain due to the nonlinear effect of loss rate and the coupling effect of the distribution functions. This behavior is observed in some complex fluids, such as diblock copolymer or surfactant solutions (Daniel *et al.*, 2001), biopolymer systems like dough (Phan-Thien *et al.*, 1998; 2000), xanthan gum solutions (Hyun *et al.*, 2002), emulsion of immiscible mixtures (Mason *et al.*, 1997; Bower *et al.*, 1999), fumed silica suspensions (Raghavan and Khan, 1997; Yziquel *et al.*, 1999), and the electrorheological fluids like a suspension of acid alumina particles in poly (dimethylsiloxane) under the electric field (Dealy and Wissbrun, 1990).

Type D (The storage modulus overshoot and the loss modulus undershoot)

When τ and frequency are large irrespective of the creation rate parameters, the effective storage modulus G' has an overshoot but the effective loss modulus G" decreases and increases as shown in Fig. 5. The phase behavior of type D is compared with type B in Fig. 6, which shows the phase diagram of the stress and the strain in reduced units.

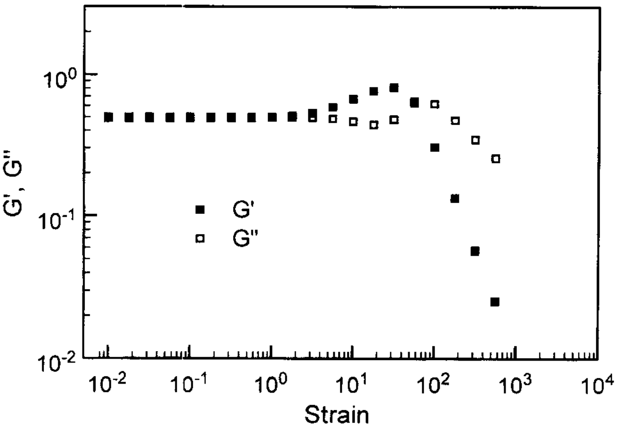

Fig. 5. Type D (with parameter set α_0=5, α_1=1, τ=1.0, at frequency=0.02).

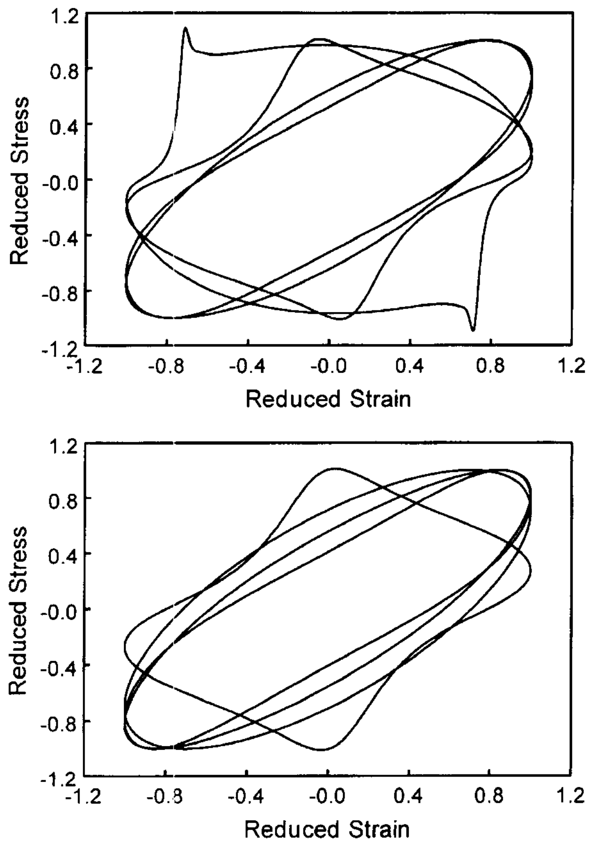

Fig. 6. Phase diagram of stress and strain for type B (upper) and type D (lower). As strain amplitude increases, the loop goes outward for type B showing the viscoelastic behavior, while it shrinks inward and then goes outward for type D.

For type B, the stress signal is partially in phase with the imposed strain and shows an elliptical orbit at small strain. As the strain increases, the orbit grows outward and becomes non-elliptic. This means that the stress signal is no longer sinusoidal in time domain because of the higher harmonic contributions to the stress signal. This behavior is well known in the literature. However unlike type B, the orbit of type D shrinks inward from the outer elliptical orbit, and the stress signal becomes partially in phase with the imposed strain. The orbit then stretches outward, and the stress signal becomes out of phase with the imposed strain at large strain amplitude. The phase diagram indicates that the material have strong elasticity at an intermediate strain and recovers the viscoelastic properties over a critical strain. The high frequency and relaxation time means that the material is more solidlike. However, the effective storage and loss moduli always decrease due to the nonlinear effect of loss rate at larger strain amplitudes. The behavior of this type has rarely been reported. Similar behavior was observed in the blend of Hyaluronate and PVA (polyvinyl alcohol)-borax in our experiments, where both G' and G" show the minimum and maximum. However only G" shows such a behavior in this type, and the mechanism is quite different. In the case of biopolymer blends, the contribution from each component is simply added with a small amount of interactions. We may find this kind of materials near future, but as of now we will exclude this type in classifying the complex fluids.

Frequency sweep

At low frequency, the effective storage modulus increases in proportion to the square of frequency and the loss modulus proportional to frequency. It is typical in the linear viscoelastic behavior. As the frequency increases over the crossover point, the loss modulus decreases and reaches a plateau and then decreases again as shown in Fig. 7. This behavior seems to follow the two-mode Maxwell model. This is because the model has two distribution functions, both for active and pendent chains, and the stress is the sum of two contributions. We separated the contribution of active and pendent chains in Fig. 8. The effective storage

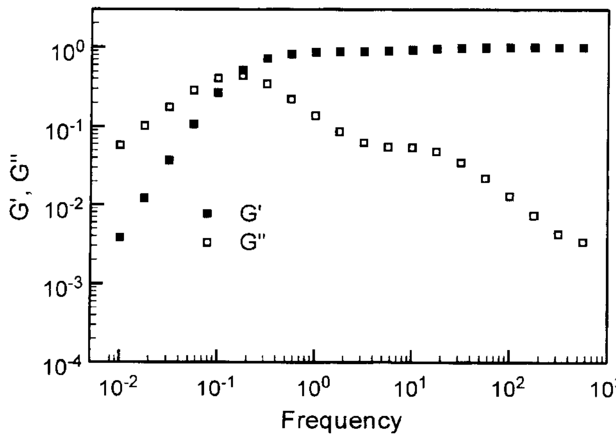

Fig. 7. Storage and loss moduli as functions of frequency for type B (with parameter set α_0=1, α_1=5, τ=0.01).

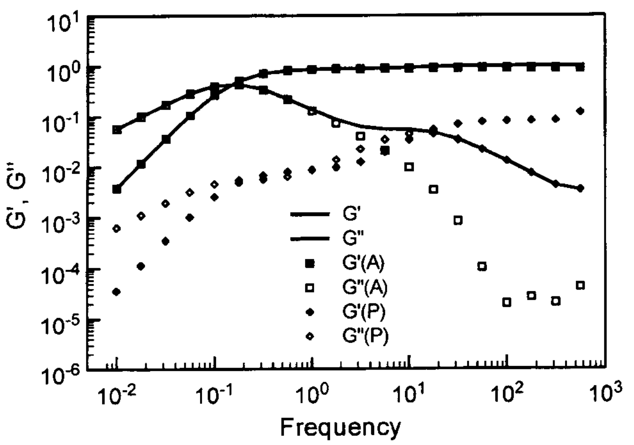

Fig. 8. Storage and loss moduli as functions of frequency for type B, with contributions from active (A) and pendent (P) chains.

modulus is dominated by the contribution of active chains. However, it becomes complicated in the case of loss modulus. At low frequencies, the contribution of active chain is dominant, but the high frequency behavior is dominated by the contribution of pendent chain. That is, the pendent chains contribute to the viscous properties at high frequencies or the response at short time intervals. This complicates the response of the material, leading to a bimodal shape in the loss modulus. We have considered the behavior of active and pendent chains independently. The frequency sweep result of active chain shows a typical viscoelastic behavior, while that of pendent chain causes a plateau region at intermediate frequencies, leading to a bimodal shape. This behavior is also observed in polymer mixtures with different molecular weight distributions (Ferry, 1980).

4. Conclusions

We have investigated the LAOS behavior of the Marrucci model, which was originally developed to describe the system of associating telechelic polymers. The model predicts three types of LAOS behavior: type A; strain thinning (G' and G" decreasing), type B; strong strain overshoot (G' and G" increasing followed by decreasing), type C; weak strain overshoot (G' decreasing, G" increasing followed by decreasing). Type D looks unphysical. We could explain the strain overshoot behavior in terms of the balance between the creation and loss rates. In type B, the creation rate becomes larger as the strain amplitude increases, and the loss rate increases too. As a result of the balance between the creation and loss rates, there appears an overshoot at intermediate strain amplitude. In type C, the creation rate has a weaker dependence of strain amplitude than the case of type B, and the creation rate increases slowly while the loss rate increases faster than the creation rate, leading to an overshoot of G" only. Compared with the experimental observation of Hyun *et al.* (2002), the types of LAOS behavior predicted by this model does not show the strain hardening behavior because of the FENE type nonlinear effect of loss rate. However, the model predicts all the other types of LAOS behavior.

Acknowledgement

The authors wish to acknowledge the Korean Science and Engineering Foundation (KOSEF) for the financial support through the Applied Rheology Center, an official engineering research center (ERC) in Korea.

References

Ahn, K. H. and K. Osaki, 1995, Mechanism of shear thickening investigated by a network model, *J. Non-Newtonian Fluid Mech.* **56**, 267-288.

Bird, R. B., C. F. Curtiss, R. C. Armstrong and O. Hassager, 1987, Dynamics of polymeric liquids, vol. 2, 2nd Ed., John Wiley & Sons, New York, Chapter 20.

Daniel, C., I. W. Hamley, M. Wilhelm and W. Mingvanish, 2001, Non-linear rheology of a face-centered cubic phase in a diblock copolymer gel, *Rheol. Acta* **40**, 39-48.

Dealy, J. M. and K. F. Wissbrun, 1990, Melt rheology and its role in plastics processing: Theory and applications, VNR, New York, Chapter 5.

Ferry, J. D., 1980, Viscoelastic properties of polymers, 3rd Ed., John Wiley & Sons, New York, Chapter 13.

Giacomin, J. A. and J. G. Oakley, 1992, Structural network models for molten plastics evaluated in large amplitude oscillatory shear, *J. Rheol.* **36**, 1529-1546.

Giacomin, A. J. and J. M. Dealy, 1993, Large-amplitude oscillatory shear in A. A. Collyer (Ed.), Techniques in rheological measurement, Chapman and Hall, London, Chapter 4.

Hyun, K., S. H. Kim, K. H. Ahn and S. J. Lee, 2002, Large amplitude oscillatory shear as a way to classify the complex fluids, submitted to the *J. Non-Newtonian Fluid Mech.*

Larson, R. G., 1999, The structure and rheology of complex fluids, Oxford University Press, New York.

Macosko, C. W., 1994, Rheology: Principles, measurements, and applications, VCH, New York.

Mason, T. G., M. Lacasse, G. S. Grest, D. Levine, J. Bibette and D. A. Weitz, 1997, Osmotic pressure and viscoelastic shear moduli of concentrated emulsions, *Phys. Rev. E* **56**, 3150-3166.

Phan-Thien, N. and M. Safari-Ardi, 1998, Linear viscoelastic properties of flour-water doughs a different water concentrations, *J. Non-Newtonian Fluid Mech.* **74**, 137-150.

Phan-Thien, N., M. Newberry and R. I. Tanner, 2000, Non-linear oscillatory flow of a solid-like viscoelastic material, *J. Non-Newtonian Fluid Mech.* **92**, 67-80.

Raghavan, S. R. and S. A. Khan, 1997, Shear-thickening response of fumed silica suspensions under steady and oscillatory shear, *J. Colloid and Interface Sci.* **185**, 57-67.

See, H., 2001, Advances in measuring linear viscoelastic properties using novel deformation geometries and Fourier transform techniques, *Korea-Australia Rheology J.* **13**, 67-81.

Tirtaatmadja, V., K. C. Tam and R. D. Jenkins, 1997, Superposition of oscillations on steady shear flow as a technique for investigating the structure of associative polymers, *Macromolecules* **30**, 1426-1433.

Vaccaro, A. and G. Marrucci, 2000, A model for the nonlinear rheology of associating polymers, *J. Non-Newtonian Fluid Mech.* **92**, 261-273.

Wilhelm, M., D. Maring and H. spies, 1998, Fourier-transform rheology, *Rheol. Acta* **37**, 399-405.

Wilhelm, M., P. Reinheimer and M. Ortseifer, 1999, High sensitivity Fourier-transform rheology, *Rheol. Acta* **38**, 349-356.

Wilhelm, M., P. Reinheimer, M. Ortseifer, T. Neidhöfer and H. Spiess, 2000, The crossover between linear and non-linear mechanical behaviour in polymer solutions as detected by Fourier-transform rheology, *Rheol. Acta* **39**, 241-246.

Yosick, J. A. and A. J. Giacomin, 1996, Can nonlinear deformation amplify subtle differences in linear viscoelasticity?, *J. Non-Newtonian Fluid Mech.* **66**, 193-212.

Yosick, J. A., A. J. Giacomin and P. Moldenaers, 1997, A kinetic network model for nonlinear flow behavior of molten plastics in both shear and extension, *J. Non-Newtonian Fluid Mech.* **70**, 103-123.

Yziquel, E., P. J. Carreau and P. A. Tanguy, 1999, Non-linear viscoelastic behavior of fumed silica suspensions, *Rheol. Acta* **38**, 14-25.